

Dissipation induced extended-localized transition

Yaru Liu,¹ Zeqing Wang,¹ Chao Yang,^{2,3,4} Jianwen Jie,^{5,*} and Yucheng Wang^{2,3,4,†}

¹Department of Physics, Renmin University of China, Beijing 100872, China

²Shenzhen Institute for Quantum Science and Engineering,

Southern University of Science and Technology, Shenzhen 518055, China

³International Quantum Academy, Shenzhen 518048, China

⁴Guangdong Provincial Key Laboratory of Quantum Science and Engineering,

Southern University of Science and Technology, Shenzhen 518055, China

⁵Shenzhen Key Laboratory of Ultraintense Laser and Advanced Material Technology,

Center for Advanced Material Diagnostic Technology, and College of Engineering Physics,

Shenzhen Technology University, Shenzhen 518118, China

Mobility edge (ME), representing the critical energy that distinguishes between extended and localized states, is a key concept in understanding the transition between extended (metallic) and localized (insulating) states in disordered and quasiperiodic systems. Here we explore the impact of dissipation on a quasiperiodic system featuring MEs by calculating steady-state density matrix and analyzing quench dynamics with sudden introduction of dissipation, and demonstrate that dissipation can lead the system into specific states predominantly characterized by either extended or localized states, irrespective of the initial state. Our results establish the use of dissipation as a new avenue for inducing transitions between extended and localized states, and for manipulating dynamic behaviors of particles.

Introduction.— The investigation of electronic transport properties lies at the heart in condensed-matter physics [1]. Disorder is ubiquitous, and its crucial impact on transport properties was unveiled through Anderson localization (AL) [2, 3]. In three-dimensional systems with substantial disorder, a transition can occur from the extended phase to the localized phase. Near this transition point, mobility edges (MEs) may emerge, defining the critical energy that distinguishes extended states from localized ones [3–5]. ME is a vital focus in studying disordered materials and helps in understanding a material’s conductivity and electronic properties. If the Fermi energy is within the localized region, conductivity at zero temperature disappears, whereas in the extended region it results in finite zero-temperature conductivity. Therefore, changing the Fermi energy’s position across the ME can cause the extended (metal)-localized (insulator) transition. In addition to random disorder, quasiperiodic potentials can also induce the extended-localized transition (ELT) [6–22], resulting in distinct physical phenomena different from that of disordered potentials. For instance, in one-dimensional (1D) quasiperiodic systems, the ELT and MEs can exist, whereas in disordered systems, these phenomena are expected to occur in dimensions higher than two according to scaling theory [23].

With advancements in non-Hermitian physics and the manipulation of both dissipation and quantum coherence in experimental settings, recent years have witnessed a growing interest in studying dissipative open quantum systems. Dissipation can profoundly change the properties of quantum systems, leading to various types of phase transitions [24–34]. The impact of dissipation on localization has also garnered considerable attention [35–44]. It’s worth noting that dissipation can reduce coherence, thereby disrupting or even destroying AL [35–40], which

arises from quantum interference. On the other hand, certain types of dissipation can drive AL into a stable state that retains its localized properties without being destroyed [42, 43]. However, all previous studies on the impact of dissipation on localization did not involve MEs. When considering MEs, a natural and fundamental question arises: what physical phenomena will emerge from the interplay of dissipation and MEs?

In this letter, we investigate the impact of dissipation on a 1D quasiperiodic system with exact MEs and find that the dissipation can drive the system into specific states, which may be extended or localized, regardless of the initial state. In other words, dissipation can induce transitions not only from localized states to extended states but also from extended states to localized states in a system with MEs, revealing that dissipation not only disrupts localization but can also lead to localization. Remarkably, the ELT here does not necessitate the change in either disorder strength or particle density, both of which are believed to be the ways for altering the properties of extension and localization through shifting the relative positions of the Fermi surface and the ME. Thus, the combination of dissipation and MEs results in novel and rich physical phenomena and provides a new approach to manipulate transport properties of particles.

Model.— We consider a dissipative system whose density matrix ρ follows the Lindblad master equation [45, 46],

$$\frac{d\rho(t)}{dt} = \mathcal{L}[\rho(t)] = -i[H, \rho(t)] + \mathcal{D}[\rho(t)]. \quad (1)$$

where \mathcal{L} is referred to as the Lindbladian, with its dissipative component denoted as,

$$\mathcal{D}[\rho(t)] = \sum_j \Gamma_j \left(O_j \rho O_j^\dagger - 1/2 \{O_j^\dagger O_j, \rho\} \right), \quad (2)$$

which contains a set of jump operators O_j with the corresponding strength Γ_j . Assuming that \mathcal{L} is time-independent, we can express $\rho(t) = e^{\mathcal{L}t}\rho(0)$. One can define the steady state as $\rho_{ss} = \lim_{t \rightarrow \infty} \rho(t)$, which corresponds to the eigenstate of the Lindblad generator with zero eigenvalue, i.e., $\mathcal{L}[\rho_{ss}] = 0$.

The Hamiltonian we consider in Eq. (1) is denoted as

$$H = J \sum_{j=1} \left(c_j^\dagger c_{j+1} + \text{h.c.} \right) + 2 \sum_{j=1} V_j n_j, \quad (3)$$

where c_j and $n_j = c_j^\dagger c_j$ are respectively the annihilation operator and local number operator at site j , and J is the nearest neighbor hopping coefficient. The local potential V_j takes $V \cos[2\pi\omega j + \theta]$ for even sites and vanishes for odd sites, where ω is an irrational number, V and θ are potential amplitude and phase offset, respectively. The model is referred to as the 1D quasiperiodic mosaic model, which features two MEs at $E_c = \pm J/V$ [13]. This model has been recently realized, and the MEs have been successfully detected [47]. Without loss of generality, we set $J = 1$, $V = 1$, $\theta = 0$ and $\omega = (\sqrt{5} - 1)/2$.

The jump operator considered in Eq. (2) is given by [42, 43, 48–52]

$$O_j = (c_j^\dagger + e^{i\alpha} c_{j+l}^\dagger)(c_j - e^{i\alpha} c_{j+l}), \quad (4)$$

which acts on a pair of sites j and $j+l$. This jump operator does not alter the system's particle number, but it does change the relative phase between the pair of sites with the distance l . For example, this operator synchronizes them from an out-of-phase (in-phase) mode to an in-phase (out-of-phase) mode when the dissipative phase α is set to 0 (π). Such property is important for attaining the intended extended or localized stationary states, as will become evident below.

Dissipation induced ELT.— We begin by examining the jump operators in Eq. (4) for $l = 1$ and analyze the properties of the stationary solution ρ_{ss} for Eq. (1) in the eigenbasis of the Hamiltonian H . Unless otherwise stated, we set $\rho_0 = \rho_{L+1} = 0$ at the boundaries with L being the system size. Fig. 1(a-c) illustrate the transition of the system's steady state from being predominantly occupied by high-energy localized states to predominantly occupied by low-energy localized states as the dissipation phase is varied from $\alpha = 0$ to $\alpha = \pi$. We emphasize that the steady state here is independent of the initial state. This implies that if the initial state is within the extended region located in the middle of the energy spectrum, when the jump operator with $\alpha = 0$ or $\alpha = \pi$ is introduced, the state will ultimately predominantly occupy localized regions.

The occupation of the above-mentioned steady states can be understood by analyzing the relative phases of neighboring lattice sites. For an arbitrary n -th eigenstate of the Hamiltonian H , we can calculate the number of in-phase site pairs $N_{n,l}^{\text{in}}$ with distance l , and its proportion

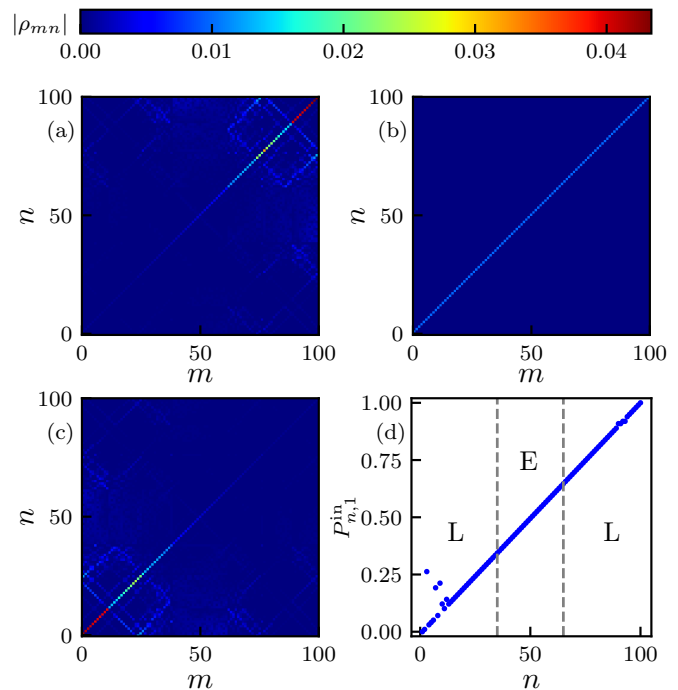


Figure 1: The absolute values of the density matrix elements for steady states with the dissipative phases (a) $\alpha = 0$, (b) $\alpha = \pi/2$, and (c) $\alpha = \pi$ in the eigenbasis of Hamiltonian given in Eq. (3). (d) The proportion of in-phase lattice site pairs for each eigenstate. Dashed lines mark the MEs, separating eigenstates into localized (L), extended (E), and localized (L) regions as eigenvalues increase. Here we take $l = 1$, $L = 100$ and $\Gamma = 1$.

$P_{n,l}^{\text{in}} = N_{n,l}^{\text{in}}/N_t$, where $N_t = L - l$ represents the total number of site pairs. Fig. 1(d) illustrates that eigenstate with higher (lower) energy tends to have larger (smaller) $P_{n,1}^{\text{in}}$, explaining why the steady state predominantly occupies high-energy (low-energy) localized eigenstates for $\alpha = 0$ ($\alpha = \pi$). Thus, α plays an important role in driving the quantum system into specific states.

We further investigate the effect of the jump operators in Eq. (4) with $l = 2$. Based on the aforementioned physical picture, we calculate the proportion of in-phase lattice site pairs $P_{n,2}^{\text{in}}$, as shown in Fig. 2(a), and find that it exhibits a V-shaped pattern. It can be observed that the localized states on both sides of the eigenenergy spectrum tend to have more symmetric in-phase site pairs, while the extended states in the middle of the spectrum tend to have more asymmetric out-of-phase site pairs. Therefore, by appropriately choosing the dissipation phase α , it is possible to control whether the system's steady state predominantly occupies localized eigenstates or extended eigenstates, as demonstrated in Fig. 2(b-d). When the dissipative phase is $\alpha = 0$ [Fig. 2(b)], the system is expected to reach a steady state predominantly occupied by states associated with symmetric in-phase site pairs, thus primarily occupying

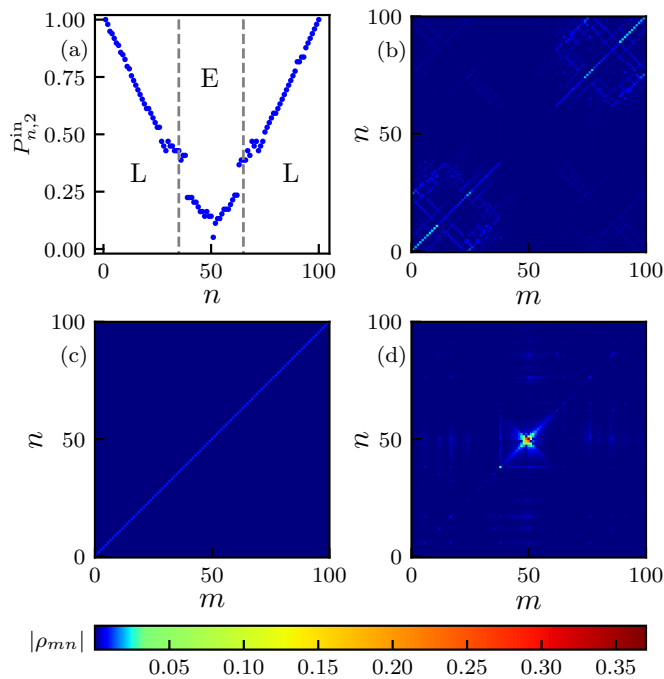


Figure 2: (a) The proportion of in-phase lattice site pairs for each eigenstate, with the mobility edges marked by the dashed lines. Like in Fig. 1, the dashed lines here represent MEs. The absolute values of the steady-state density matrix elements with the dissipative phases (b) $\alpha = 0$, (c) $\alpha = \pi/2$, and (d) $\alpha = \pi$ in the eigenbasis of Hamiltonian H . Other parameters are $l = 2$, $L = 100$ and $\Gamma = 1$.

the localized eigenstates in both higher-energy and lower-energy regions. Conversely, when $\alpha = \pi$ [Fig. 2(d)], the system is anticipated to attain a steady state mainly occupied by states linked to asymmetric out-of-phase site pairs, favoring the occupation of extended eigenstates in the mid-energy regions. When $\alpha = \pi/2$ [Fig. 2(c) and Fig. 1(b)], the dissipation operator becomes Hermitian, leading to the system reaching the maximally-mixed state $(\rho_{ss})_{mn} = \delta_{mn}/L$ as its steady state. For arbitrary α , we can calculate the percentage of localized eigenstates and extended eigenstates in steady states, defined by $P_l = N_l/L$ ($P_e = N_e/L$) with N_l (N_e) being the number of the localized (extended) eigenstates, as shown in Fig. 3(a). When α is tuned from 0 to π , the system's steady state shows the transition from being dominated by localized eigenstates to being dominated by extended eigenstates, which indicates that dissipation can be used to manipulate the ELT.

We further examine this transition from a dynamical perspective. We prepare a localized or extended eigenstate as the initial state and introduce dissipation with $l = 2$ at $t = 0$. We then calculate the fidelity, which represents the overlap between the time-evolved state $\rho(t)$ and the initial state ρ_i , denoted as [53, 54]

$$F[\rho(t), \rho_i] = \text{Tr}[\sqrt{\rho(t)^{1/2} \rho_i \rho(t)^{1/2}}]. \quad (5)$$

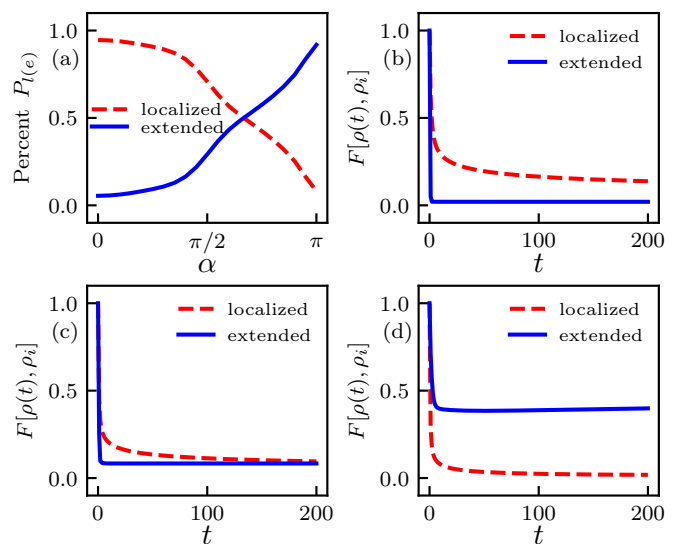


Figure 3: (a) The percentage of localized eigenstates (P_l) and extended eigenstates (P_e) in steady states as a function of the dissipative phase α , and the results are size-independent. Evolution of the fidelity defined in Eq. (5) after a sudden introduction of dissipation with the strength $\Gamma = 1$ and the phases (b) $\alpha = 0$, (c) $\alpha = \pi/2$, and (d) $\alpha = \pi$. The initial states are set as follows: the system's ground state, which is localized (red dashed line), and the state corresponding to the eigenvalue situated in the center of the energy spectrum of the Hamiltonian H , characterized as extended (blue solid line). Here, $L = 144$ and $l = 2$.

At $\alpha = 0$ [Fig. 3(b)], the fidelity rapidly approaches zero when the initial state is extended, indicating that the structure of the initial state has been completely modified. Conversely, the fidelity tends to a non-zero value when the initial state is localized, suggesting that certain characteristics of the initial state are preserved. This is because the steady state is primarily occupied by localized states. When $\alpha = \pi/2$ [Fig. 3(c)], the steady state contains extended and localized states, resulting in non-zero fidelity for both. Finally, for $\alpha = \pi$ [Fig. 3(d)], the steady state primarily consists of extended states. Therefore, when the initial state is in an extended state, the fidelity is not equal to zero, but it tends to zero when the initial state is a localized state.

We have revealed that an extended (localized) state can be guided towards a steady state primarily composed of localized (extended) states by applying dissipation. Furthermore, even after removing the dissipation once the system has reached a steady state, its properties will persist. This differs from the majority of previous studies on the influence of dissipation on AL, where the introduction of dissipation disrupts localization, but removing it leads the disordered system back to localization. By introducing a period of dissipation and subsequently removing it, the system's Hamiltonian remains unchanged, but the state properties undergo a profound transforma-

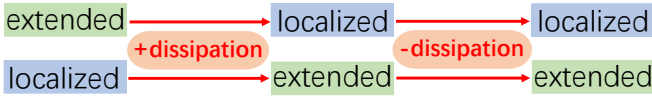


Figure 4: Schematic illustrating transitions between extended and localized states manipulated by dissipation.

tion, as showed in Fig. 4. Consequently, dissipation provides a means to manipulate transitions between localized and extended states.

Experimental realization.— In Ref. [13], the authors have proposed a highly feasible experimental setup to realize the quasiperiodic mosaic model based on optical Raman lattices [55–58]. They constructed a spin-1/2 system using two hyperfine states $|\uparrow\rangle = |F_1, m_{F1}\rangle$ and $|\downarrow\rangle = |F_2, m_{F2}\rangle$, and mapped the spin-up (spin-down) lattice sites to the odd (even) sites [see Fig. 5]. They applied the Raman coupling via a standing wave field and a plane wave to generate the spin-dependent primary lattice $V_p(x)\sigma_z = V_1 \cos(2k_p x + \phi_p)\sigma_z$, and three standing wave fields together to generate a secondary quasiperiodic lattice $V_s(x) = V_2 \cos(2k_s x + \phi_s)$ only for spin-down atoms. As the depth of the primary lattice significantly exceeds that of the secondary lattice ($V_1 \gg V_2$), we will proceed to discuss the realization of the dissipation operator below, with the secondary lattice’s impact considered negligible. We will primarily focus on discussing the realization of the case with $\alpha = 0$ by introducing the auxiliary lattice [48–51]. An arbitrary phase α can be achieved, for instance, through an array of resonators coupled by superconducting qubits [42, 52].

Fig. 5(a) shows the realization of the pairwise dissipator with $l = 1$. By coherently coupling two nearly degenerate levels in the system to an auxiliary site in between with antisymmetric Rabi frequencies $\pm\Omega$, which can be obtained by controlling the wavelength of the driving laser to match that of the primary lattice, one can achieve the annihilation part of the dissipative operator. Decay back to the lower sites occurs through spontaneous emission, and this process is isotropic, leading to the form of the creation operator being symmetric [48–51]. In this way, one can realize the jump operator of the form $(c_j^\dagger + c_{j+1}^\dagger)(c_j - c_{j+1})$.

Similarly, the case for $l = 2$ can also be realized, as shown in Fig. 5(b). However, there are several key differences with the case of $l = 1$. (1) The auxiliary lattice must be spin-dependent, necessitating the use of two hyperfine states $|\uparrow\rangle = |F'_1, m'_{F1}\rangle$ and $|\downarrow\rangle = |F'_2, m'_{F2}\rangle$ to construct a spin-1/2 lattice. It is essential to ensure that they satisfy the condition $m_{F1} - m'_{F1} = m_{F2} - m'_{F2}$. (2) It requires a phase difference of π with the primary lattice, namely that the odd (even) sites correspond to spin-down (spin-up) sites in the auxiliary lattice. (3) By manipulating the polarization of the driving laser, one can attain the specific coupling that spin-up (spin-down)

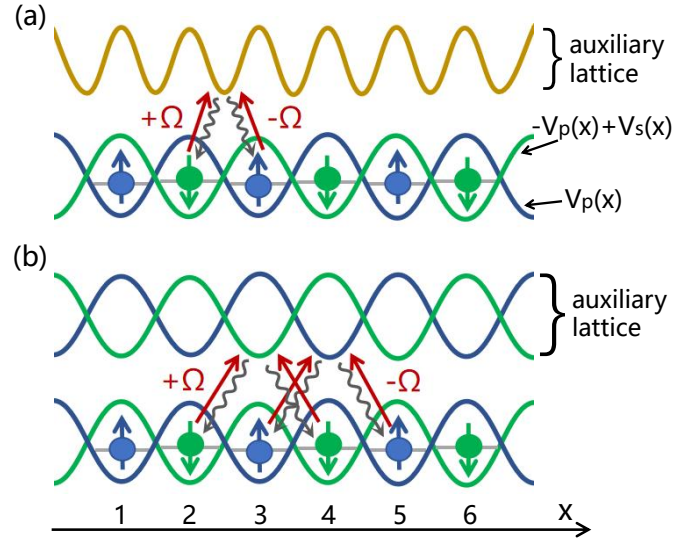


Figure 5: Schematic realization of the dissipative process of the form $(c_j^\dagger + c_{j+l}^\dagger)(c_j - c_{j+l})$ with (a) $l = 1$ and (b) $l = 2$. The lower (upper) lattice correspond to the physical (auxiliary) lattice. Atoms in the lower sites are coupled to the auxiliary sites in between with opposite Rabi frequency $\pm\Omega$, and then spontaneously decay back to the lower sites.

states in the primary lattice only couple with spin-up (spin-down) states in the auxiliary lattice [59, 60]. For example, if $m_{F1} - m'_{F1} = 0$, the driving laser needs to be π -polarized [61, 62]. Moreover, to obtain a π phase shift in the effective Rabi frequency Ω from one spin-up (spin-down) site to the next spin-up (spin-down), one need to set the driving laser’s wavelength to be twice that of the standing wave laser generating the primary lattice.

By comparing the diffusion [63–66] or transport behaviors [15, 67–69] of atoms before and after the introduction of dissipation, one can obtain extended and localized information about the initial and final states, thereby detecting the ELT caused by dissipation.

Conclusion and Discussion.— We have investigated the influence of dissipation on the 1D quasiperiodic mosaic model, which possesses exact MEs, and have proposed its experimental realization. By calculating the distribution of the density matrix of the steady states and the characteristics of quench dynamics with sudden introduction of dissipation, we revealed that dissipation can drive the system into specific states primarily occupied by either extended or localized states, without regard to the initial states. Hence, dissipation can be utilized to induce transitions between extended (metallic) states and localized (insulating) states, thereby enabling the manipulation of particle transport behaviors. In addition to its applications in condensed matter physics, controlling particles into specific states also has potential applications in quantum simulation. For instance, when simulating systems with MEs using cold atoms,

preparing atoms near the ground state is challenging because these states are localized, which is unfavorable for precise measurements of certain properties. However, as we mentioned, introducing dissipation can help prepare atoms near the ground state.

The manipulation of the ELT essentially relies on the distinct phases of individual states and is expected to be common in various systems featuring MEs [see supplementary materials [70]]. Our results pose several interesting issues deserving further investigation. In particular, how does the combination of the dissipation with a many-body system featuring MEs influence the system? Can the dissipation be employed to manipulate the transitions between thermalized states and many-body localized states? Further, can the similar ETL exist in a three dimensional dissipative disordered system with MEs? These issues are important and warrant further exploration in next studies.

We thank Long Zhang, Xin-Chi Zhou, Shi Yu, and Bing Yang for valuable discussions. This work was supported by the National Natural Science Foundation of China (Grant No. 12104210, Grant No. 12104205), National Key R&D Program of China under Grant No.2022YFA1405800, the Shenzhen Science and Technology Program (Grant No. ZDSYS20200811143600001) and the Natural Science Foundation of Top Talent of SZTU(GDRC202202). Y. Liu acknowledges support from the Fundamental Research Funds for the Central Universities, and the Research Funds of Renmin University of China (22XNH100).

* Corresponding author: Jianwen.Jie1990@gmail.com

† Corresponding author: wangyc3@sustech.edu.cn

- [1] A. Lagendijk, B. Tiggele, and D. S. Wiersma, Fifty years of Anderson localization, *Phys. Today* **62**, 24 (2009).
- [2] P. W. Anderson, *Phys. Rev.* **109**, 1492 (1958).
- [3] P. A. Lee and T. V. Ramakrishnan, Disordered electronic systems, *Rev. Mod. Phys.* **57**, 287 (1985).
- [4] F. Evers and A. D. Mirlin, Anderson transitions, *Rev. Mod. Phys.* **80**, 1355 (2008).
- [5] B. Kramer and A. MacKinnon, Localization: theory and experiment, *Rep. Prog. Phys.* **56**, 1469 (1993).
- [6] G. Roati, C. D'Errico, L. Fallani, M. Fattori, C. Fort, M. Zaccanti, G. Modugno, M. Modugno, and M. Inguscio, Anderson localization of a non-interacting Bose-Einstein condensate, *Nature (London)* **453**, 895 (2008).
- [7] C. M. Soukoulis and E. N. Economou, Localization in One-Dimensional Lattices in the Presence of Incommensurate Potentials, *Phys. Rev. Lett.* **48**, 1043 (1981).
- [8] S. Das Sarma, S. He, and X. C. Xie, Mobility edge in a model one-dimensional potential, *Phys. Rev. Lett.* **61**, 2144 (1988).
- [9] J. Biddle, B. Wang, D. J. Priour Jr, and S. Das Sarma, Localization in one-dimensional incommensurate lattices beyond the Aubry-André model, *Phys. Rev. A* **80**, 021603 (2009); J. Biddle and S. Das Sarma, Predicted mobility edges in one-dimensional incommensurate optical lattices: an exactly solvable model of Anderson localization, *Phys. Rev. Lett.* **104**, 070601 (2010).
- [10] X. Li, X. Li, and S. Das Sarma, Mobility edges in one dimensional bichromatic incommensurate potentials, *Phys. Rev. B* **96**, 085119 (2017).
- [11] H. Yao, H. Khoudli, L. Bresque, and L. Sanchez-Palencia, Critical behavior and fractality in shallow one-dimensional quasiperiodic potentials, *Phys. Rev. Lett.* **123**, 070405 (2019).
- [12] S. Ganeshan, J. H. Pixley, and S. Das Sarma, Nearest neighbor tight binding models with an exact mobility edge in one dimension, *Phys. Rev. Lett.* **114**, 146601 (2015).
- [13] Y. Wang, X. Xia, L. Zhang, H. Yao, S. Chen, J. You, Q. Zhou, and X.-J. Liu, One dimensional quasiperiodic mosaic lattice with exact mobility edges, *Phys. Rev. Lett.* **125**, 196604 (2020).
- [14] X.-C. Zhou, Y. Wang, T.-F. J. Poon, Q. Zhou, and X.-J. Liu, Exact new mobility edges between critical and localized states, arXiv:2212.14285.
- [15] Y. Wang, L. Zhang, W. Sun, T.-F. J. Poon, and X.-J. Liu, Quantum phase with coexisting localized, extended, and critical zones, *Phys. Rev. B* **106**, L140203 (2022).
- [16] T. Liu, X. Xia, S. Longhi, L. Sanchez-Palencia, Anomalous mobility edges in one-dimensional quasiperiodic models, *SciPost Phys.* **12**, 027 (2022).
- [17] S. Longhi, Topological phase transition in non-Hermitian quasicrystals, *Phys. Rev. Lett.* **122**, 237601 (2019); S. Longhi, Metal-insulator phase transition in a non-Hermitian Aubry-André-Harper Model, *Phys. Rev. B* **100**, 125157 (2019); S. Longhi, Non-Hermitian control of localization in mosaic photonic lattices, arXiv:2310.02334.
- [18] H. Jiang, L.-J. Lang, C. Yang, S.-L. Zhu, and S. Chen, Interplay of non-Hermitian skin effects and Anderson localization in non-reciprocal quasiperiodic lattices, *Phys. Rev. B* **100**, 054301 (2019); Y. Liu, Y. Wang, X.-J. Liu, Q. Zhou, and S. Chen, Exact mobility edges, PT-symmetry breaking and skin effect in one-dimensional non-Hermitian quasicrystals, *Phys. Rev. B* **103**, 014203 (2021).
- [19] M. Gonçalves, B. Amorim, E. V. Castro, and P. Ribeiro, Hidden dualities in 1D quasiperiodic lattice models, *SciPost Phys.* **13**, 046 (2022); M. Gonçalves, B. Amorim, E. V. Castro, and P. Ribeiro, Renormalization-Group Theory of 1D quasiperiodic lattice models with commensurate approximants, *Phys. Rev. B* **108**, L100201 (2023); M. Gonçalves, B. Amorim, E. V. Castro, and P. Ribeiro, Critical phase dualities in 1D exactly-solvable quasiperiodic models, arXiv:2208.07886.
- [20] H. P. Lüschen, S. Scherg, T. Kohlert, M. Schreiber, P. Bordia, X. Li, S. D. Sarma, and I. Bloch, Single-particle mobility edge in a one-dimensional quasiperiodic optical lattice, *Phys. Rev. Lett.* **120**, 160404 (2018); T. Kohlert, S. Scherg, X. Li, H. P. Lüschen, S. D. Sarma, I. Bloch, and M. Aidelsburger, Observation of many-body localization in a one-dimensional system with single-particle mobility edge, *Phys. Rev. Lett.* **122**, 170403 (2019).
- [21] F. A. An, E. J. Meier, and B. Gadway, Engineering a flux-dependent mobility edge in disordered zigzag chains, *Phys. Rev. X* **8**, 031045 (2018); F. A. An, K. Padavić, E. J. Meier, S. Hegde, S. Ganeshan, J. H. Pixley, S. Vishveshwara, and B. Gadway, Observation of tunable mobility edges in generalized Aubry-André lattices, *Phys. Rev. Lett.* **126**, 040603 (2021).
- [22] Y. Wang, J.-H. Zhang, Y. Li, J. Wu, W. Liu, F. Mei, Y.

- Hu, L. Xiao, J. Ma, C. Chin, and S. Jia, Observation of Interaction-Induced Mobility Edge in an Atomic Aubry-André Wire, *Phys. Rev. Lett.* **129**, 103401 (2022).
- [23] E. Abrahams, P. W. Anderson, D. C. Licciardello, and T. V. Ramakrishnan, Scaling theory of localization: Absence of quantum diffusion in two dimensions, *Phys. Rev. Lett.* **42**, 673 (1979).
- [24] T. Prosen and I. Pižorn, Quantum Phase Transition in a Far-from-Equilibrium Steady State of an XY Spin Chain, *Phys. Rev. Lett.* **101**, 105701 (2008).
- [25] H. T. Mebrahtu, I. V. Borzenets, H. Zheng, Y. V. Bomze, A. I. Smirnov, S. Florens, H. U. Baranger, and G. Finkelstein, Observation of Majorana quantum critical behaviour in a resonant level coupled to a dissipative environment, *Nat. Phys.* **9**, 732 (2013); H. T. Mebrahtu, I. V. Borzenets, D. E. Liu, H. Zheng, Y. V. Bomze, A. I. Smirnov, H. U. Baranger, and G. Finkelstein, Quantum phase transition in a resonant level coupled to interacting leads, *Nature* **488**, 61 (2012).
- [26] M. V. Medvedyeva, M. T. Čubrović, S. Kehrein, Dissipation-induced first-order decoherence phase transition in a noninteracting fermionic system, *Phys. Rev. B* **91**, 205416 (2015).
- [27] K. Shastri and Francesco Monticone, Dissipation-induced topological transitions in continuous Weyl materials, *Phys. Rev. Research* **2**, 033065 (2020).
- [28] M. Oriente, T. L. Heugel, K. Arimitsu, R. Chitra, and O. Zilberberg, Distinctive class of dissipation-induced phase transitions and their universal characteristics, *Phys. Rev. Research* **3**, 023100 (2021).
- [29] K. Yamamoto, M. Nakagawa, N. Tsuji, M. Ueda, and N. Kawakami, Collective Excitations and Nonequilibrium Phase Transition in Dissipative Fermionic Superfluids, *Phys. Rev. Lett.* **127**, 055301 (2021).
- [30] W. Nie, M. Antezza, Y.-X. Liu, F. Nori, Dissipative Topological Phase Transition with Strong System-Environment Coupling, *Phys. Rev. Lett.* **127**, 250402 (2021).
- [31] K. Kawabata, T. Numasawa, and S. Ryu, Entanglement Phase Transition Induced by the Non-Hermitian Skin Effect, *Phys. Rev. X* **13**, 021007 (2023).
- [32] E. I. R. Chiacchio, A. Nunnenkamp, and M. Brunelli, Nonreciprocal Dicke Model, *Phys. Rev. Lett.* **131**, 113602 (2023).
- [33] L.-N. Wu, J. Nettersheim, J. Feß, A. Schnell, S. Burgardt, S. Hiebel, D. Adam, A. Eckardt, and A. Widera, Dynamical phase transition in an open quantum system, arXiv:2208.05164.
- [34] R. Kuzmin, N. Mehta, N. Grabon, R. A. Mencia, A. Burshtein, M. Goldstein, and V. E. Manucharyan, Observation of the Schmid-Bulgadaev dissipative quantum phase transition, arXiv:2304.05806.
- [35] S. A. Gurvitz, Delocalization in the Anderson Model due to a Local Measurement, *Phys. Rev. Lett.* **85**, 812 (2000).
- [36] B. Nowak, J. J. Kinnunen, M. J. Holland, and P. Schlagheck, Delocalization of ultracold atoms in a disordered potential due to light scattering, *Phys. Rev. A* **86**, 043610 (2012).
- [37] K. Rayanov, G. Radons, and S. Flach, Decohering localized waves, *Phys. Rev. E* **88**, 012901 (2013).
- [38] A. G. Yamilov, R. Sarma, B. Redding, B. Payne, H. Noh, and H. Cao, Position-Dependent Diffusion of Light in Disordered Waveguides, *Phys. Rev. Lett.* **112**, 023904 (2014).
- [39] M. Balasubrahmaniyam, S. Mondal, and S. Mujumdar, Necklace-State-Mediated Anomalous Enhancement of Transport in Anderson-Localized non-Hermitian Hybrid Systems, *Phys. Rev. Lett.* **124**, 123901 (2020).
- [40] S. Weidemann, M. Kremer, S. Longhi, and A. Szameit, Coexistence of dynamical delocalization and spectral localization through stochastic dissipation, *Nat. Photon.* **15**, 576 (2021).
- [41] D. A. Huse, R. Nandkishore, F. Pietracaprina, V. Ros, and A. Scardicchio, Localized systems coupled to small baths: From Anderson to Zeno, *Phys. Rev. B* **92**, 014203 (2015).
- [42] I. Yusipov, T. Lapyteva, S. Denisov, and M. Ivanchenko, Localization in Open Quantum Systems, *Phys. Rev. Lett.* **118**, 070402 (2017).
- [43] O. S. Vershinina, I. I. Yusipov, S. Denisov, M. V. Ivanchenko, T. V. Lapyteva, Control of a single-particle localization in open quantum systems, *Europhys. Lett.* **119**, 56001 (2017); I. I. Yusipov, T. V. Lapyteva, M. V. Ivanchenko, Quantum jumps on Anderson attractors, *Phys. Rev. B* **97**, 020301 (2018); I. Vakulchyk, I. Yusipov, M. Ivanchenko, S. Flach, and S. Denisov, Signatures of many-body localization in steady states of open quantum systems, *Phys. Rev. B* **98**, 020202(R) (2018).
- [44] S. Longhi, Anderson Localization in Dissipative Lattices, *Ann. Phys.* **535**, 2200658 (2023)
- [45] G. Lindblad, On the generators of quantum dynamical semigroups, *Commun. Math. Phys.* **48**, 119 (1976).
- [46] H.-P. Breuer and F. Petruccione, *The Theory of Open Quantum Systems* (Oxford University Press, Oxford, 2002).
- [47] J. Gao, I. M. Khaymovich, X.-W. Wang, Z.-S. Xu, A. Iovan, G. Krishna, A. V. Balatsky, V. Zwiller, and A. W. Elshaari, Experimental probe of multi-mobility edges in quasiperiodic mosaic lattices, arXiv:2306.10829.
- [48] S. Diehl, A. Micheli, A. Kantian, B. Kraus, H. P. Büchler, and P. Zoller, Quantum states and phases in driven open quantum systems with cold atoms, *Nat. Phys.* **4**, 878 (2008).
- [49] B. Kraus, H. P. Büchler, S. Diehl, A. Kantian, A. Micheli, and P. Zoller, Preparation of entangled states by quantum Markov processes, *Phys. Rev. A* **78**, 042307 (2008).
- [50] S. Diehl, A. Tomadin, A. Micheli, R. Fazio, and P. Zoller, Dynamical Phase Transitions and Instabilities in Open Atomic Many-Body Systems, *Phys. Rev. Lett.* **105**, 015702 (2010); S. Diehl, E. Rico, M. A. Baranov, P. Zoller, Topology by Dissipation in Atomic Quantum Wires, *Nat. Phys.* **7**, 971 (2011).
- [51] C.-E. Bardyn, M. A. Baranov, C. V. Kraus, E. Rico, A. Imamoglu, P. Zoller, S. Diehl, Topology by dissipation, *New J. Phys.* **15**, 085001 (2013).
- [52] D. Marcos, A. Tomadin, S. Diehl, and P. Rabl, Photon condensation in circuit quantum electrodynamics by engineered dissipation, *New J. Phys.* **14**, 055005 (2012).
- [53] M. Nielsen and I. Chuang, *Quantum Computation and Quantum Information* (Cambridge University Press, 2000).
- [54] P. Zanardi, H. T. Quan, Xiaoguang Wang, and C. P. Sun, Mixed-state fidelity and quantum criticality at finite temperature, *Phys. Rev. A* **75**, 032109 (2007).
- [55] X.-J. Liu, Z.-X. Liu, and M. Cheng, Manipulating topological edge spins in a one-dimensional optical lattice, *Phys. Rev. Lett.* **110**, 076401 (2013); X.-J. Liu, K. T. Law, and T. K. Ng, Realization of 2D spin-orbit interaction and exotic topological orders in cold atoms, *Phys. Rev. Lett.*

- 112**, 086401 (2014).
- [56] B. Song, L. Zhang, C. He, T. F. J. Poon, E. Hajiyev, S. Zhang, X.-J. Liu, and G.-B. Jo, Observation of symmetry-protected topological band with ultracold fermions, *Sci. Adv.* **4**, eaao4748 (2018); B. Song, C. He, S. Niu, L. Zhang, Z. Ren, X.-J. Liu, and G.-B. Jo, Observation of nodal-line semimetal with ultracold fermions in an optical lattice, *Nat. Phys.* **15**, 911 (2019).
- [57] L. Zhang and X.-J. Liu, spin orbit coupling and topological phases for ultracold atoms. arXiv:1806.05628.
- [58] Z. Wu, L. Zhang, W. Sun, X.-T. Xu, B.-Z. Wang, S.-C. Ji, Y. Deng, S. Chen, X.-J. Liu, and J.-W. Pan, Realization of two-dimensional spin-orbit coupling for Bose-Einstein condensates, *Science* **354**, 83 (2016); Z.-Y. Wang, X.-C. Cheng, B.-Z. Wang, J.-Y. Zhang, Y.-H. Lu, C.-R. Yi, S. Niu, Y. Deng, X.-J. Liu, S. Chen, and J.-W. Pan, Realization of ideal Weyl semimetal band in ultracold quantum gas with 3D spin-orbit coupling, *Science* **372**, 271 (2021).
- [59] E. Arimondo, M. Inguscio, and P. Violino, Experimental determinations of the hyperfine structure in the alkali atoms, *Rev. Mod. Phys.* **49**, 31 (1977).
- [60] D. Budker, W. Gawlik, D. F. Kimball, S. M. Rochester, V. V. Yashchuk, and A. Weis, Resonant nonlinear magneto-optical effects in atoms, *Rev. Mod. Phys.* **74**, 1153 (2002).
- [61] A. Jenkins, J. W. Lis, A. Senoo, W. F. McGrew, and A. M. Kaufman, Ytterbium Nuclear-Spin Qubits in an Optical Tweezer Array, *Phys. Rev. X* **12**, 021027 (2022).
- [62] N. Chen, L. Li, W. Huie, M. Zhao, I. Vetter, C. H. Greene, and J. P. Covey, Analyzing the Rydberg-based optical-metastable-ground architecture for ^{171}Yb nuclear spins, *Phys. Rev. A* **105**, 052438 (2022).
- [63] R. Ketzmerick, K. Kruse, S. Kraut, and T. Geisel, What determines the spreading of a wave packet?, *Phys. Rev. Lett.* **79**, 1959 (1997).
- [64] M. Larcher, F. Dalfovo, and M. Modugno, Effects of interaction on the diffusion of atomic matter waves in one-dimensional quasiperiodic potentials, *Phys. Rev. A* **80**, 053606 (2009).
- [65] Y. Wang, L. Zhang, S. Niu, D. Yu, and X.-J. Liu, Realization and detection of non-ergodic critical phases in optical Raman lattice, *Phys. Rev. Lett.* **125**, 073204 (2020).
- [66] T. Shimasaki, M. Prichard, H. E. Kondakci, J. E. Pagett, Y. Bai, P. Dotti, A. Cao, T.-C. Lu, T. Grover, and D. M. Weld, Anomalous localization and multifractality in a kicked quasicrystal, arXiv:2203.09442.
- [67] M. Saha, S. K. Maiti, A. Purkayastha, Anomalous transport through algebraically localized states in one-dimension, *Phys. Rev. B* **100**, 174201 (2019).
- [68] J.-P. Brantut, J. Meineke, D. Stadler, S. Krinner, and T. Esslinger, Conduction of ultracold fermions through a mesoscopic channel, *Science* **337**, 1069 (2012).
- [69] C.-C. Chien, S. Peotta, and M. D. Ventura, Quantum transport in ultracold atoms, *Nat. Phys.* **11**, 998 (2015).
- [70] See Supplemental Material for details on (I) the impact of dissipation on another 1D system with exact MEs; (II) dissipation induced critical-localized transition. The Supplemental Materials includes the references [12, 14].

Supplementary Material: Dissipation induced extended-localized transition

In the Supplementary Materials, we discuss the impact of dissipation on two systems with exact mobility edges (MEs). The first system has the traditional ME that separates extended states from localized ones, allowing dissipation to induce the transitions between extended and localized states. The second system features a new ME that separates critical states from localized states, enabling dissipation to induce the critical-localized transition.

We first consider the following model [S1]

$$H_1 = t_1 \sum_{j=1} (c_j^\dagger c_{j+1} + \text{h.c.}) + 2\lambda \sum_{j=1} \frac{\cos(2\pi\omega j + \delta)}{1 - \beta \cos(2\pi\omega j + \delta)} n_j, \quad (\text{S1})$$

where ω is an irrational number, t_1 , λ , and β ($\beta \in (-1, 1)$) represent the hopping strength, the on-site modulation strength, and the deformation parameter, respectively. The exact expression of its ME is [S1]

$$E_{1c} = 2\text{sgn}(\lambda)(|t_1| - |\lambda|)/\beta. \quad (\text{S2})$$

We introduce the jump operators described by Eq. (4) in the main text with $l = 1$ and study the distribution of the steady-state density matrix ρ_{ss} in the eigenbasis of the Hamiltonian H_1 . As in the main text, we set $\rho_0 = \rho_{L+1} = 0$ at the boundaries, where L represents the system size. Fig. S1(a) shows the $P_{n,1}^{\text{in}} = N_{n,1}^{\text{in}}/N_t$ for each eigenstate, where $N_{n,1}^{\text{in}}$ and N_t are the number of in-phase site pairs and the total number of site pairs, respectively, with $N_t = L - 1$. Similar to Fig. 1(d) in the main text, eigenstate with higher (lower) energy tends to have larger (smaller) $P_{n,1}^{\text{in}}$. However, the localized and extended properties of this system differ from those of the model in the main text. Here, there is only one ME that separates extended states from localized states. Thus, when the dissipative phase $\alpha = 0$, the steady state predominantly occupies high-energy extended eigenstates [Fig. S1(b)], while at $\alpha = \pi$, the steady state predominantly occupies low-energy localized eigenstates [Fig. S1(c)]. For other models with MEs, we have also found that the jump operator described by Eq. (4) in the main text can manipulate the transition between extended and localized states. This demonstrates the generality of this manipulation method.

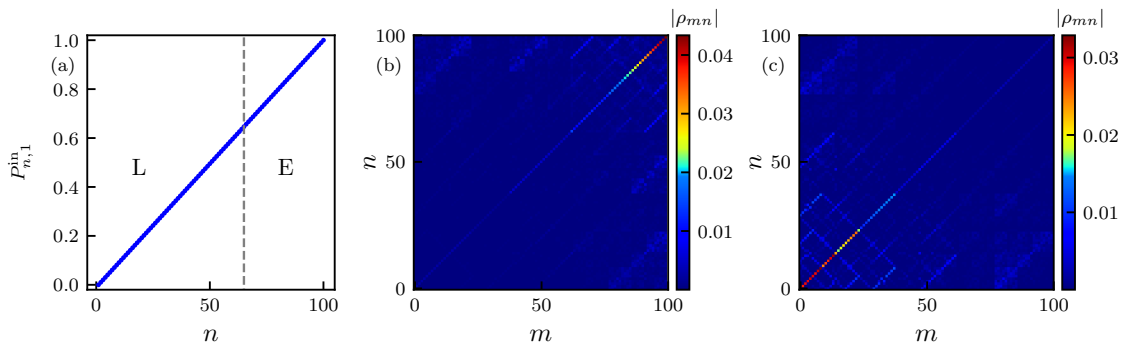


Figure S1: (a) The proportion of in-phase lattice site pairs for each eigenstate. Dashed lines are the MEs satisfying Eq. (S2), separating eigenstates into localized (L) and extended (E) regions as eigenvalues increase. The absolute values of the density matrix elements for steady states with the dissipative phases (b) $\alpha = 0$ and (c) $\alpha = \pi$ in the eigenbasis of Hamiltonian given in Eq. (S1). Here we take $t_1 = 0.8$, $\lambda = 0.825$, $\beta = -0.1$, $\delta = 0$, $\omega = (\sqrt{5} - 1)/2$, $L = 100$ and $\Gamma = 1$.

Another model we examined, which possesses precise MEs that distinguish critical and localized states, is denoted as [S2]

$$H_2 = \sum_j (t_j a_j^\dagger a_{j+1} + \text{h.c.}) + \sum_j \lambda_j n_j, \quad (\text{S3})$$

where both the on-site potential λ_j and the hopping coefficient t_j are mosaic, with

$$\{t_j, \lambda_j\} = \begin{cases} \{t_2, 2\lambda_0 \cos[2\pi\omega(j-1) + \theta]\}, & \text{mod}(j, 2) = 1, \\ 2\lambda_0 \cos(2\pi\omega j + \theta)\{1, 1\}, & \text{mod}(j, 2) = 0. \end{cases} \quad (\text{S4})$$

with t_2 and θ being hopping coefficient and phase offset, respectively. For convenience, we set $\lambda_0 = 1$, $\theta = 0$, $\omega = (\sqrt{5} - 1)/2$, and the MEs are given by

$$E_c = \pm t_2. \quad (\text{S5})$$

Similarly, we introduce the identical dissipative operators with $l = 1$ and set $\rho_0 = \rho_{L+1} = 0$ at the boundaries. Subsequently, we analyze the distribution of the steady-state density matrix ρ_{ss} in the eigenbasis of the Hamiltonian H_2 . It is evident that at $\alpha = 0$ in the dissipative phase, the steady state mainly populates high-energy localized eigenstates [Fig. S2(a)], whereas at $\alpha = \pi$, the steady state predominantly occupies mid-energy critical eigenstates [Fig. S2(b)]. Furthermore, as mentioned in the main text, for arbitrary α , we can determine the proportion of localized and critical eigenstates in the steady states. This is defined as $P_l = N_l/L$ ($P_c = N_c/L$), where N_l (N_c) represents the number of localized (critical) eigenstates, as illustrated in Fig. S2(c). As α varies from 0 to π , the system's steady state transitions from being primarily comprised of localized eigenstates to being predominantly composed of critical eigenstates. This transition highlights the potential of dissipation to manipulate the critical-localized transition.

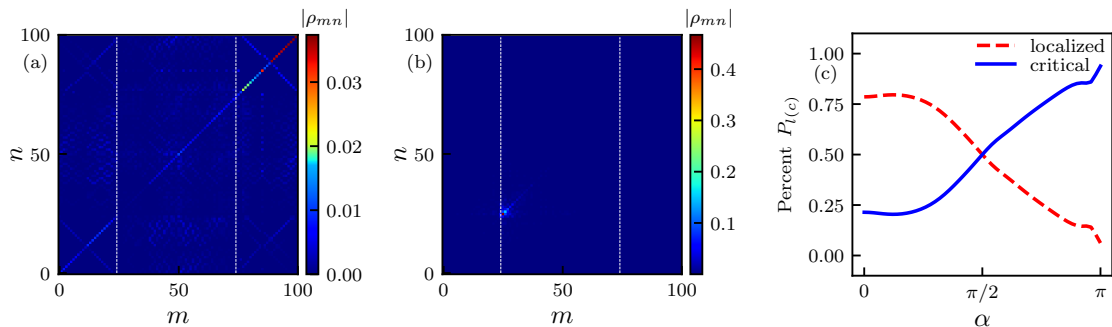


Figure S2: The absolute values of the density matrix elements for steady states with the dissipative phases (a) $\alpha = 0$ and (b) $\alpha = \pi$ in the eigenbasis of Hamiltonian given in Eq. (S3). Dashed lines are the MEs satisfying Eq. (S5), separating localized states from critical ones. (c) The percentage of localized eigenstates (P_l) and critical eigenstates (P_c) in steady states versus α , and the results are size-independent. Other parameters are $\lambda_0 = 1$, $t_2 = 1$, $\omega = (\sqrt{5} - 1)/2$, $L = 100$, $l = 1$ and $\Gamma = 1$.

* Corresponding author: Jianwen.Jie1990@gmail.com

† Corresponding author: wangyc3@sustech.edu.cn

[S1] S. Ganeshan, J. H. Pixley, and S. Das Sarma, Nearest neighbor tight binding models with an exact mobility edge in one dimension, Phys. Rev. Lett. **114**, 146601 (2015).

[S2] X.-C. Zhou, Y. Wang, T.-F. J. Poon, Q. Zhou, and X.-J. Liu, Exact new mobility edges between critical and localized states, arXiv:2212.14285.